Magnetic Doppler Imaging: numerical experiments and application to α^2 CVn

O.P. Kochukhov

Uppsala Astronomical Observatory, Box 515, SE-751 20, Uppsala, Sweden

Abstract.
Numerical experiments designed to evaluate the performance of the new Magnetic Doppler Imaging code `Invers10` are described. Numerous test runs showed that given high-resolution observations in 4 Stokes parameters the code is capable of reconstructing abundance and magnetic field vector distributions simultaneously and without any prior assumptions about magnetic field geometry. At the same time we found that in order to achieve reliable reconstruction using only circular polarization data it is necessary to impose additional constraints on the possible magnetic field geometry. We implemented those constraints in the form of a new regularization function and successfully applied modified version of the code to the Magnetic Doppler Imaging of α^2 CVn.

1. Introduction

During the last two decades Doppler Imaging has been successfully applied to the investigation of surface structures on late-type active and magnetic chemically peculiar (CP) stars. Maps of temperature and abundance distributions have beed obtained in various studies and surface inhomogeneities were studied in details unaccessible by any other technique (Strassmeier & Linsky 1996).

It is generally believed that magnetic field is responsible or at least plays an important role in the generation and evolution of stellar surface structures. However despite this common understanding very little is known about surface distributions of stellar magnetic fields. For magnetic CP stars, which have well-organized fields, only average magnetic quantities (Mathys 1993) are routinely obtained. This kind of observational data allows one to make only first crude estimate of the magnetic geometry which cannot match resolution achieved with temperature and abundance mapping. For active late-type stars the situation is even worse – complexity of their magnetic fields allowed only rough estimate of the average field strengths and filling factors from magnetic broadening or splitting of intensity line profiles (Johns-Krull & Valenti 1996), while measurements of disk-averaged polarization usually yeilded null results (Brown & Landsreet 1981).

It was realized long ago that applying Doppler Imaging method to the reconstruction of magnetic geometries helps to reach qualitatively new level of understanding of stellar magnetic fields. Piskunov (1985) and later Vasilchenko et al. (1996) developed methods for simultaneous reconstruction of magnetic field and abudance distribution for magnetic CP stars, while Semel (1989) and Donati (1999) applied Zeeman-Doppler Imaging to several late-type stars. In these pioneering studies only Stokes I and V profiles were used and a number of simplified assumptions (multipole field geometry, analytical approximation of local line profiles for magnetic CP stars or averaging many spectral lines in the weak field regime and neglecting surface temperature imhomogeneities in the magnetic imaging of late-type stars) were made. Recent improvements in the quality and quantity of spectropolarimetric data available for magnetic imaging (notably measurements of linear polarization in the line profiles by Wade et al. (1999) and comissioning of several spectropolarimetric units for high-resolution cross-dispersed echelle spectrographs) as well as steady increase of available computer power required and made possible the new generation of Magnetic Doppler Imaging (MDI) codes, capable of simultaneous accurate reconstruction of vector magnetic field and abundance or temperature distributions using temporal variation of Stokes vector. Such general MDI code `Invers10` was recently developed by Piskunov (1999 and this volume). In this paper we describe numerical testing and performance evaluation of the new code and report preliminary results of its application to one of the classical magnetic CP stars.

2. Numerical testing of MDI code

As with other applications of Doppler Imaging technique, Magnetic Doppler Imaging code requires extensive testing and evaluation of its performance.

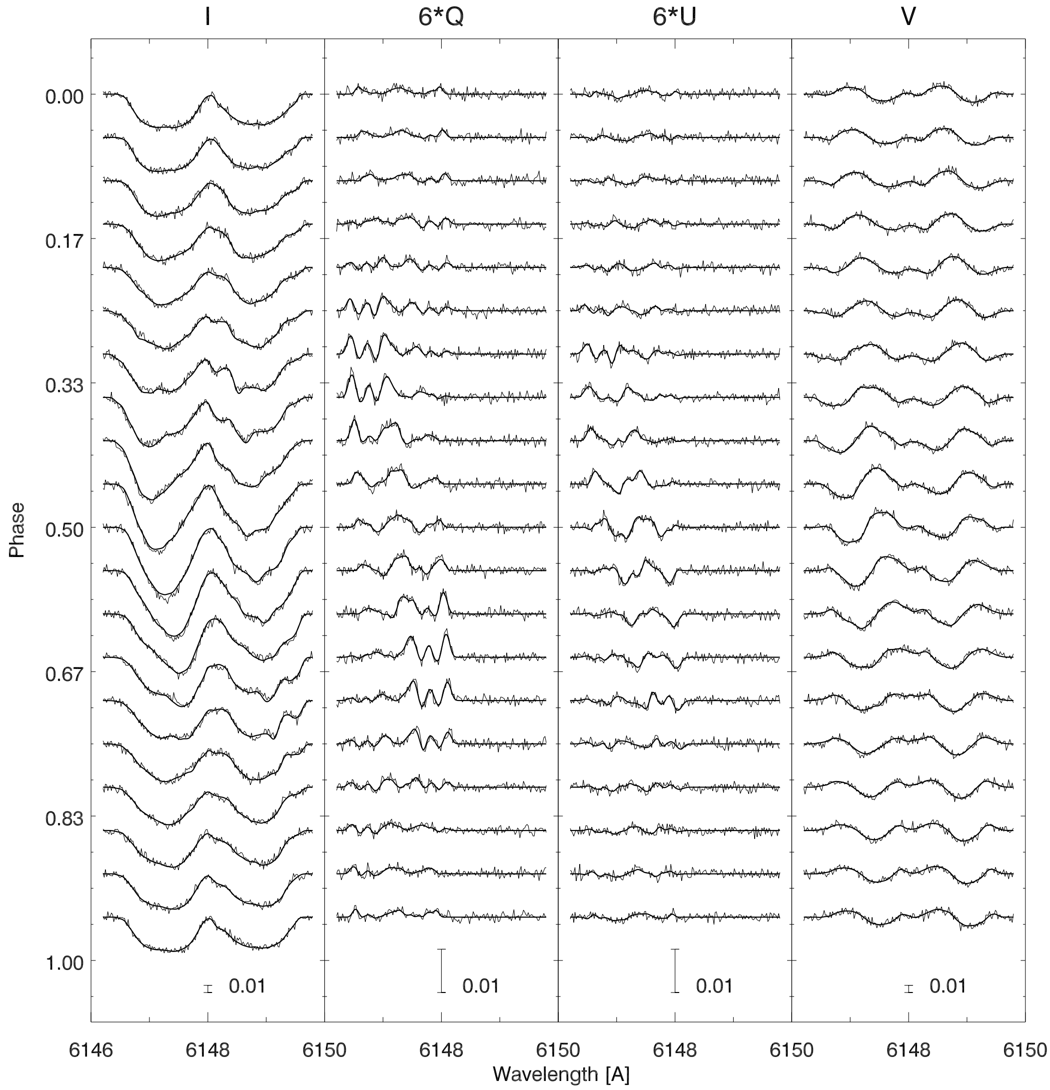

Figure 1: *Variations of Stokes I, Q, U and V profiles computed for the basic test model (Table 1). Simulated observations of Stokes profiles are shown by the thin curve. The thick curves show final fit to the Stokes vector variations achieved by the MDI code. Note the difference in scale between Stokes I, V and Stokes Q, U profiles.*

Table 1: *Setup for numerical experiments with* `Invers10` *code.*

Stellar parameters	$T_{\rm eff} = 9000$ K, $log\,{\rm g} = 4.0$, $v \sin i = 30$ km s^{-1}, $i = 60°$
Magnetic field	$H_d = 8$ kG, $\beta = 90°$
Abundance map	Single Fe abundance spot with 1.5 dex contrast
Line list	Fe II 6147.74, 6149.26 Å
Spectra	20 phases, R = 100000, SNR = 300(I,V) and 1500(Q,U)
Initial guess	zero field, homogeneous abundance distribution

This can be done with the help of numerical experiments. In this paper we describe simulations for CP stellar domain, namely for stars with inhomogeneous surface distribution of chemical elements and well-ordered, predominantly dipolar magnetic fields. In future we plan to extend our work to the late-type active stars, which have less organized fields and inhomogeneous surface temperature distribution.

We simulated observations in 4 Stokes parameters by forward modeling. Table 1 specifies basic set of parameters for the test star used in numerical experiments.

Fig. 1 shows the sample of line profiles in 4 Stokes parameters. Their variations with rotational phase of the star were computed for the basic magnetic field model described in Table 1 and for the single spot of enhanced iron abundance located on the negative magnetic pole.

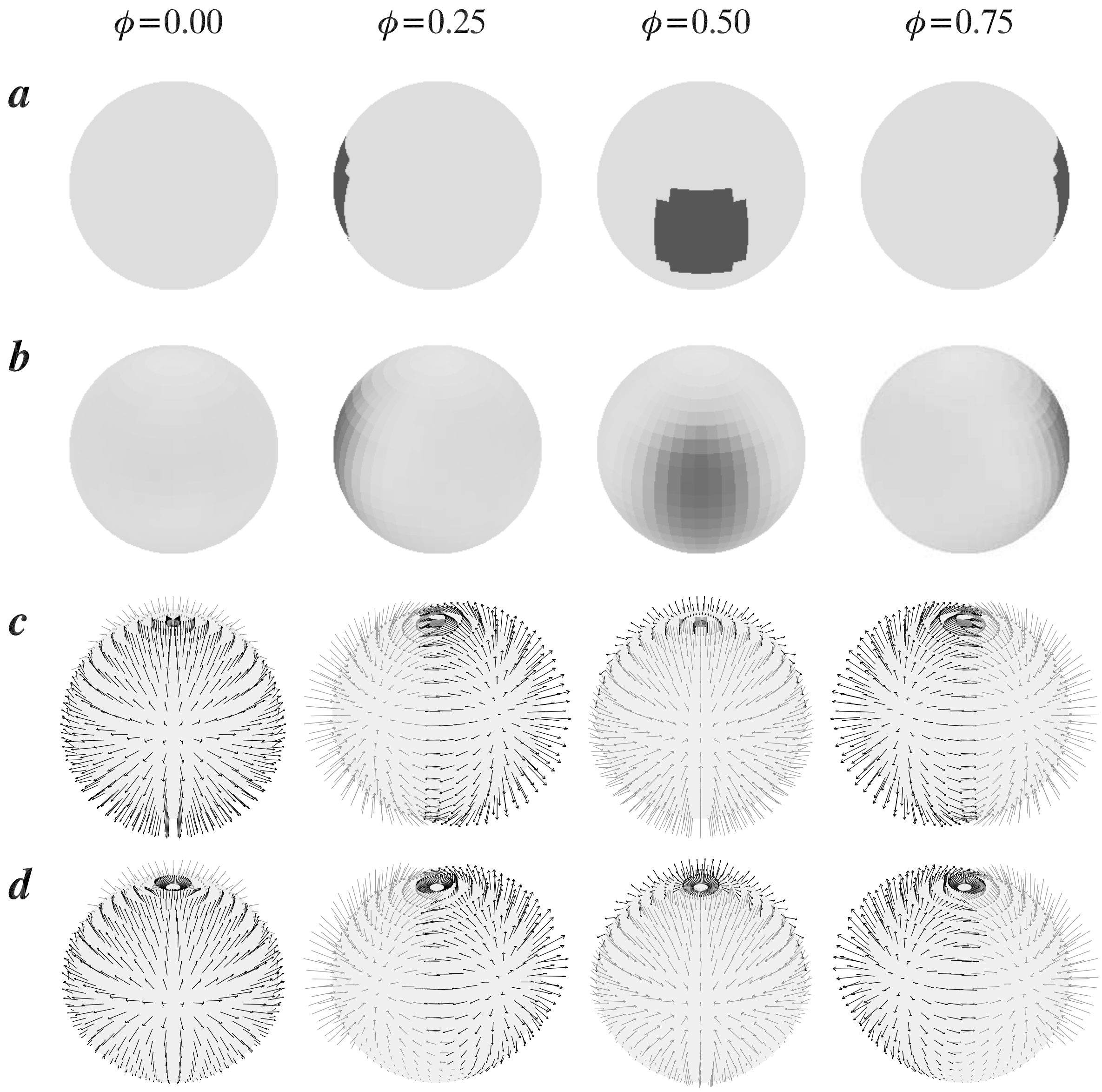

Figure 2: *Comparison of the true Fe abundance (a) and vector magnetic field (c) distributions and reconstructed maps of abundance (b) and magnetic field (d).*

Noticeble difference between variations of two Fe II lines seen in Stokes I data, reflects different magnetic sensitivity of these two lines. It is interesting to note exotic Zeeman pattern of Fe II 6149.26 Å. For this spectral feature wavelength positions of π and σ components coinside and in the case of simple Zeeman effect this leads to the absence of any linear polarization signal from this line. Results of the Magnetic Doppler Imaging reconstruction from these profiles are shown on Fig. 2. In this favourable case of large magnetically induced spectral variability, very good results were achieved, except, perhaps, for the few lowest latitudes belts, which have very little influence on the spectra and therefore retained zero initial values of the magnetic field strength. In this test the abundance distribution and all three components of the magnetic field vector were reconstructed simultaneously and self-consistently using zero-field and homogeneous abundance distribution as initial guess. In solving the inverse problem we did not use any additional assumptions about field structure.

After the first evaluation of `Invers10` performance we considered various tests in which quality of the spectra, stellar parameters and other factors were varied. As the parametric space of the possible experiments is enormous, we decided to explore the space around our basic model, not departing very far from it. In this sence testing of the MDI code was necessarily restricted. Table 2 summarizes basic types of conducted numerical tests. In the first column we list the type of experiment, what parameter was changed; second column shows amount of change with respect

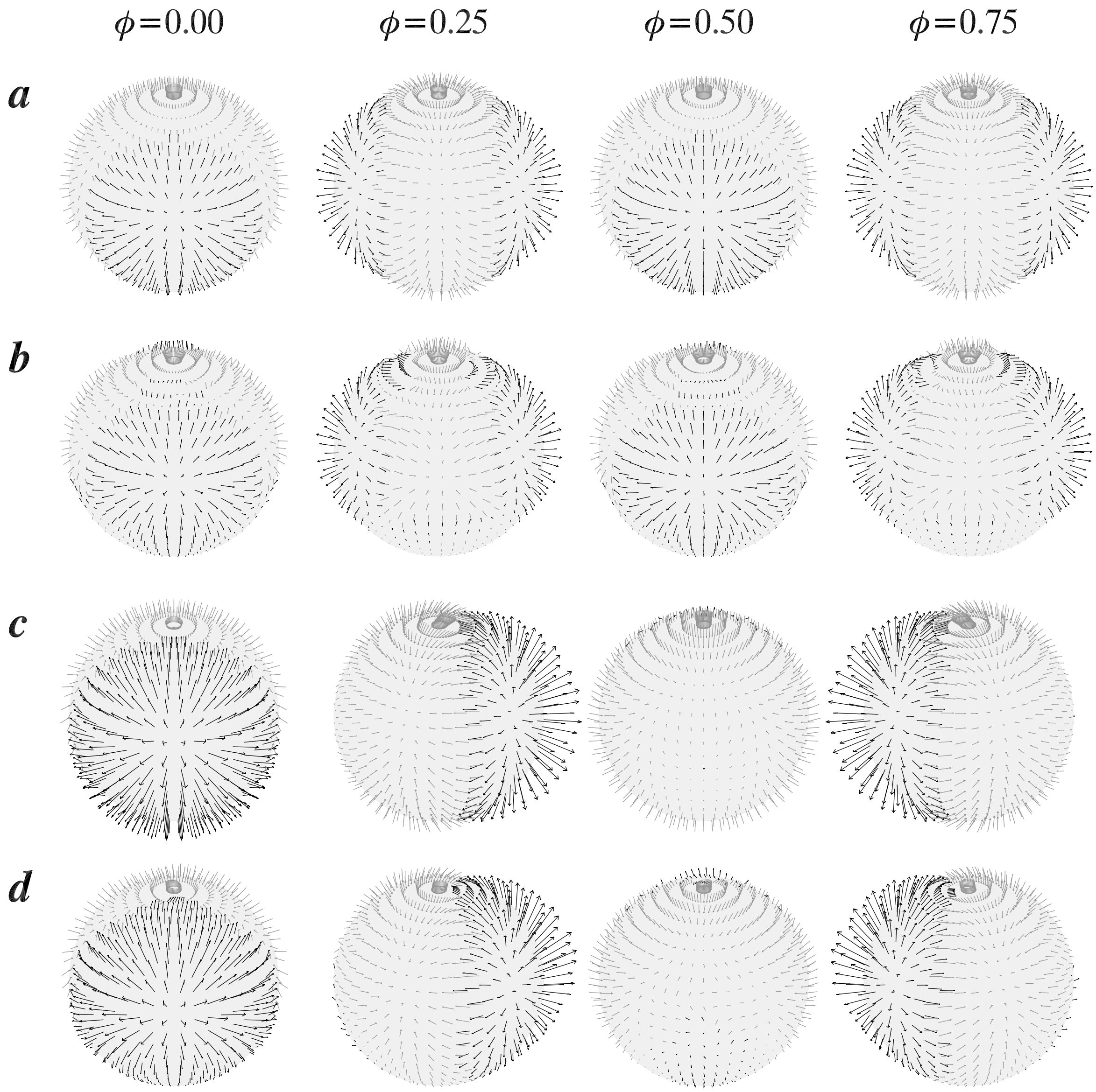

Figure 3: *Reconstruction of the complex magnetic field geometries. True maps of 8 kG quadrupole (a) and combination of 8 kG dipole and 8 kG quadrupole (c) field are compared with reconstructed (correspondingly (b) and (c)) magnetic maps.*

to the basic model and, finally, last column contains comments on the results of experiment. If abundance and magnetic maps were recovered successfully, without significant loss of information, no comment appear, otherwise two types of symbols indicate what recovering problem was detected.

Detailed discussion and quantative analysis of all numerical tests mentioned in Table 2 will be published elsewhere. In this paper we will concentrate on a few most important and interesting experiments.

Fig. 3 illustrates reconstruction of the complex magnetic field geometries. In this test we did not introduce abundance variations in the input map but still let the code vary abundance during solving inverse problem. The final abundance contrast spans only one tenth of a dex and is not shown on Fig. 3. At the same time for both 8 kG quadrupole field and a combination of aligned dipole and quadrupole (both components have polar strength of 8 kG) true field was successfully reproduced after final iteration. The latter example of the recovery of dipole plus quadrupole field is of particular interest since in this case surface variation of field modulus is very large compared to the simple dipole field. However even in this extreme case reconstructed magnetic map does not show any noticeble signs of degradation. Thus `Invers10` is not bound to the reconstruction of simple magnetic field structures.

Another interesting experiment is recovering of the magnetic field for slowly rotating stars. On Fig.

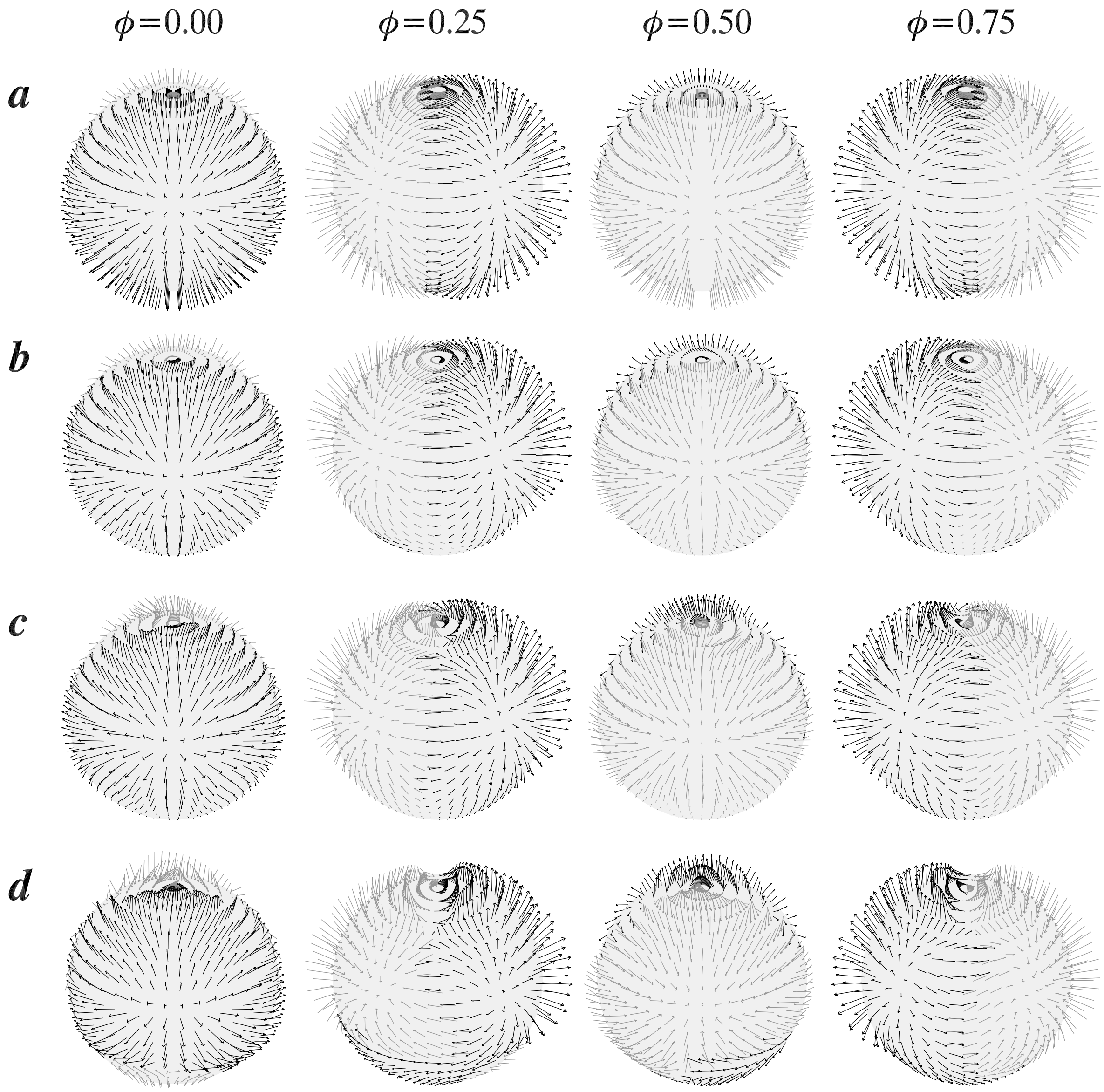

Figure 4: *Reconstruction of the magnetic field for stars with with different rotation rates. True magnetic field distribution (a) is compared with the reconstruction performed for $v \sin i$ of 30 (b), 10 (c) and 5 km s^{-1} (d).*

4 the true magnetic map and the reconstructions for $v \sin i$ of 30, 10 and 5 $\mathrm{km\,s^{-1}}$ are shown. In all these tests the abundance map consisting of several spots on different latitudes were simultaneously reconstructed from the same Stokes vector data. The quality of the field reconstruction slightly worsens with decreasing rotational velocity, but even for the slowest rotator (Fig. 4d) one can easily recognize dipolar field structure in the reconstructed magnetic map. Fig. 5 shows results for the recovering of abundance distributions for the same test runs. It is very interesting and instructive to observe the interplay between two effects used for imaging – Zeeman and Doppler shifts. For high rotational rates Doppler effect dominates and is most important for the inversion of Stokes vector, while for slow rotators domination of Zeeman effect is clearly visible. It works even for very slow $v \sin i$, when conventional Doppler Imaging is practically useless (compare Fig. 5d and e). The quality of the abundance reconstruction progressively worsens with decreasing $v \sin i$, but to a much lesser degree than in ordinary Doppler Imaging when practically all information on the latitude distribution of the abundance spots is lost. Apparently the presence of magnetic field improves recovering of abundance distribution. This becomes possible not only because of additional Zeeman shifts of local line profiles, but also due to additional informational content of V, Q and U Stokes profiles. Satisfactory results achieved in reconstruction of magnetic fields for stars with low $v \sin i$ confirmed that our MDI code can be readily applied to the imaging of magnetic fields on slow ro-

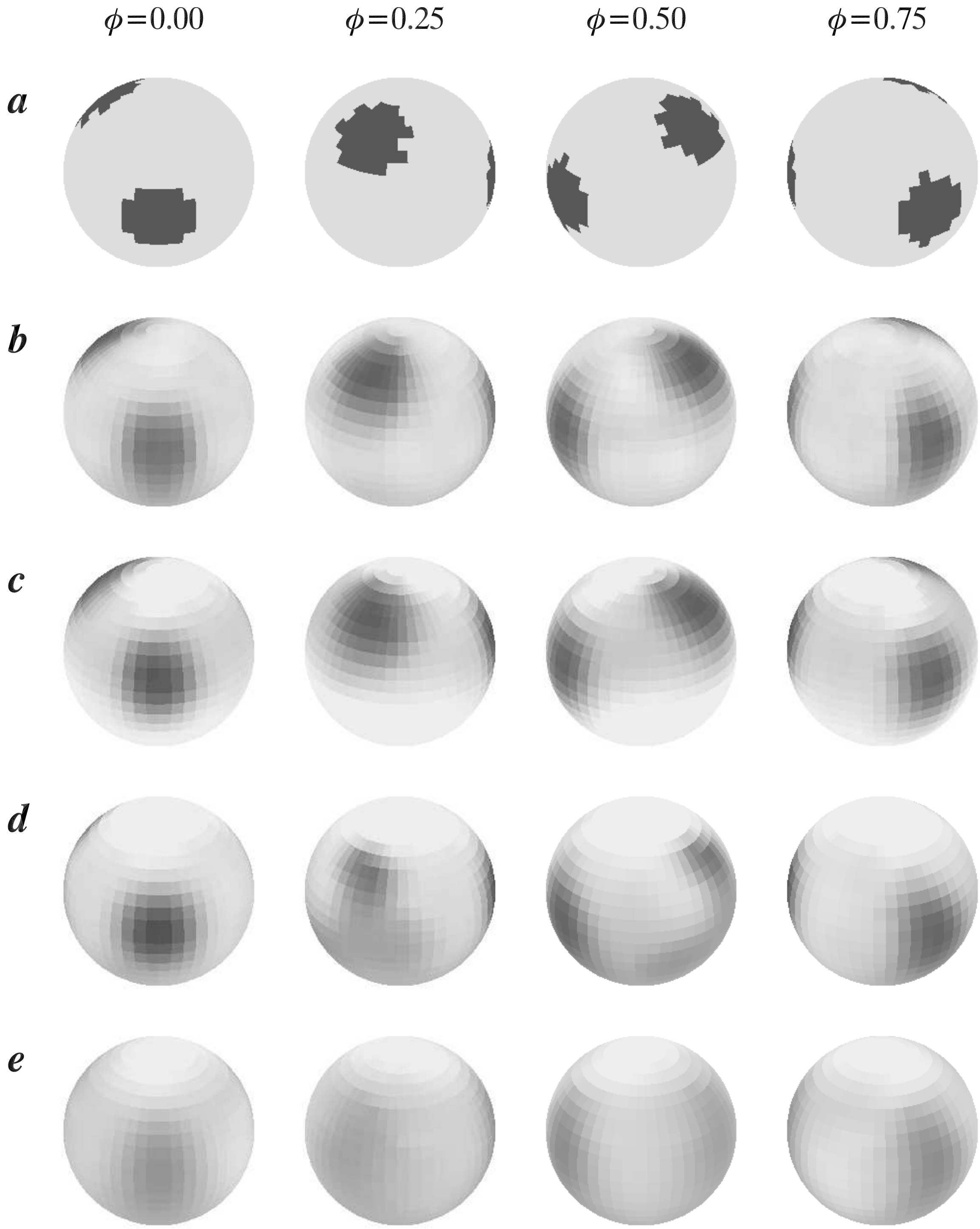

Figure 5: *Same as Fig. 4 but for Fe surface distribution. Reconstruction of abundance distribution for non-magnetic star with* $v \sin i = 5\ km\,s^{-1}$ *is also shown (e).*

tators which dominate among CP stars with strong fields.

3. IV imaging and multipolar regularization

Up to now the quality (signal-to-noise ratio and resolving power) of the existing Stokes vector observations in individual line profiles is still very limited (Wade et al. 1999). At the same time high-resolution and high signal-to-noise Stokes I and V datasets already exist for a number of CP stars or can be easily obtained. Therefore it is important to investigate the performance of `Invers10` code for IV imaging problem – reconstruction of the magnetic field without linear polarization observations. As it can be expected

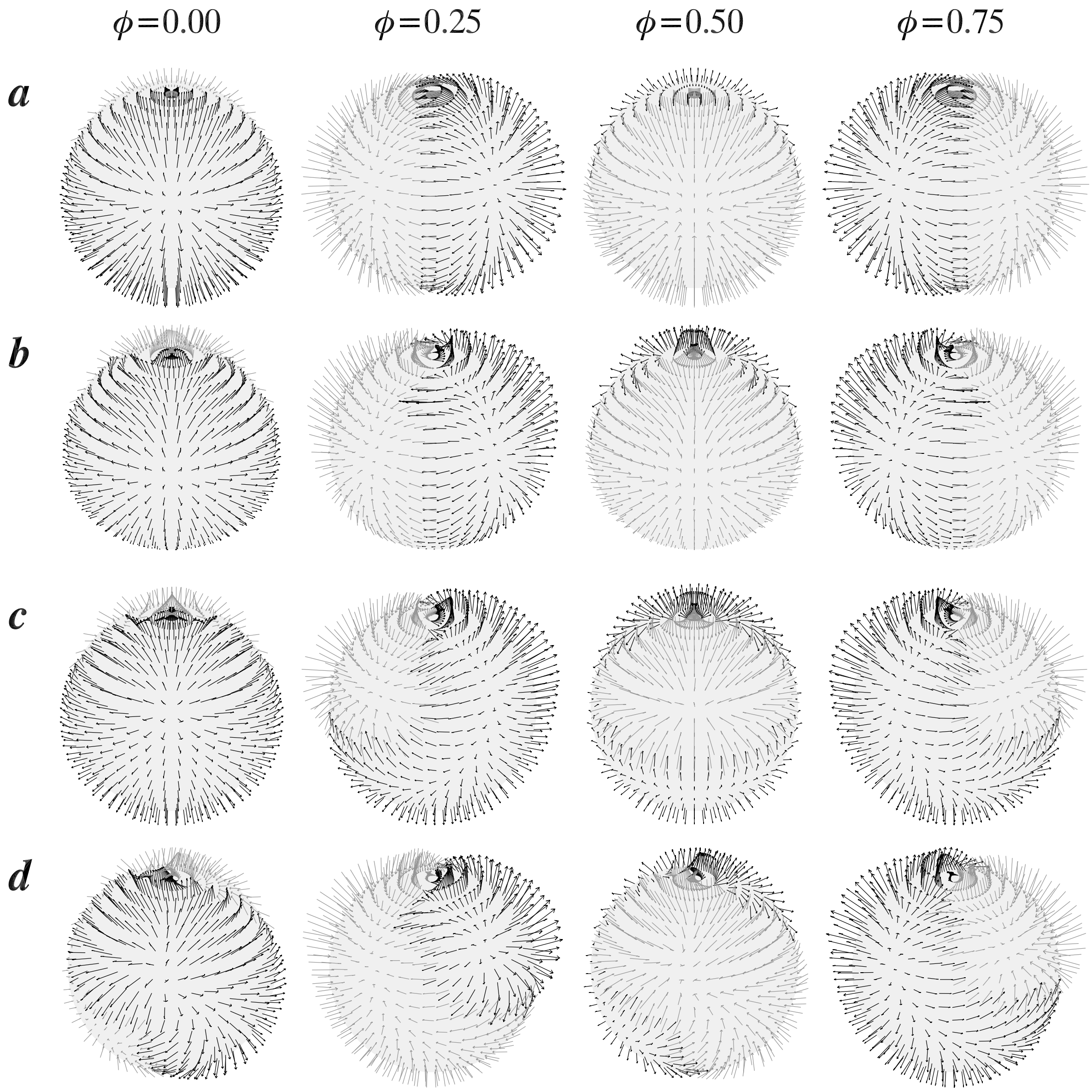

Figure 6: *Reconstruction of the magnetic field using only cilcular polarization data. True distribution (a) is compared with the reconstructions performed from zero field initial guess (b), 4 kG radial initial field and initial field in the form of 8 kG dipole rotated in the equatorial plane by 90 degrees with respect to the true magnetic geometry.*

inverse problem becomes less well-defined in this case and therefore reconstruction of the magnetic structures is much more difficult, especially when one tries to recover magnetic field using different non-zero initial guesses. Fig. 6 shows disappointing results of such test. The quality of imaging using only circular polarization data is not acceptable. As it was seen on the previous reconstructed images inversion procedure has poor sensitivity to the lower latitudes. In the case of imaging with I and V Stokes parameters this problem increases dramatically and bad reconstruction zone extends up to the stellar equator.

An obvious way of tackling this problem is to use additional information about the structure of magnetic fields on CP stars. It was shown in many previous studies that most CP stars possess well-ordered axisymmetric fields consisting of the superposition of low-order multipoles. This information could be used in the selection among possible magnetic field geometries during magnetic imaging. Regularization is a logical place to perform such a selection.

At this point we would like to clarify that the usual Tikhonov regularization method (Goncharsky et al. 1982) is not at all applicable for the reconstruction of multipolar fields. Indeed Fig. 7 shows colatitude dependence of the gradient computed for radial and meridional components of magnetic field vector. Even for the simpliest dipolar field intrinsic variations

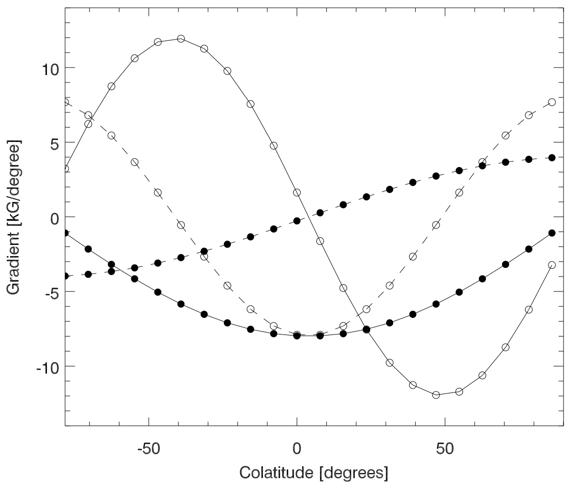

Figure 7: *Colatitude dependence of the meridional gradient computed for the radial (solid line) and meridional (dashed line) components of 8 kG dipole (filled circles) and 8 kG quadrupole (open circles) fields.*

of the gradient are relatively high and therefore minimization of the gradient will not lead to the correct solution unless, of course, the role of the regularization is small like in the imaging with complete Stokes vector data. Surface variation of the local gradient quickly increases with the departures from dipolar magnetic geometry. Therefore Tikhonov regularization method is expected to perform even worse in this case. Alternative Maximum Entropy regularization method (MEM) introduced in Doppler Imaging by Vogt et al. (1987) suffers from its own drawbacks when applied to the reconstruction of multipolar fields. MEM seeks to minimize informational content of the surface map by prohibiting large scale deviations from the average value of a parameter in interest. Thus it is not possible to apply MEM for the recovery of large scale surface variations typical for multipolar fields on CP stars. As expected, Brown et al. (1991) found that their Maximum Entropy based Zeeman-Doppler Imaging code could not reconstruct dipolar magnetic field structure using rotational modulation of I and V Stokes parameters.

Our solution to the problem of the IV imaging was to abandon Tikhonov regularization for the magnetic field and introduce instead new scheme that we call *multipolar regularization.* Below we provide brief description of the mathematical definition and implementation of the new regularization method.

MDI code solves the inverse problem by searching for the global minimum of the functional Q

$$Q = \chi^2 + \Lambda_1 F_1(A_m) + \Lambda_2 F_2(\mathbf{B}_m) \tag{1}$$

where χ^2 represents discrepancy between observed and calculated Stokes vector datasets

$$\chi^2 = \sum_\lambda \sum_\phi (\mathbf{I}^{calc}_{\lambda\phi} - \mathbf{I}^{obs}_{\lambda\phi})^2 / \sigma^2_{\lambda\phi} \tag{2}$$

A_m and $\mathbf{B}_m$ are surface abundance and magnetic field distributions, F_1 is conventional (in our case Tikhonov) regularization function neccessary for the proper recovery of abundance map, F_2 is multipolar regularization function and $\Lambda_{1,2}$ – correspondent regularization parameters. During every iteration we calculate F_2 as

$$F_2 = \sum_m \omega_m (\mathbf{B}_m - \mathbf{B}^{mod}_m)^2 \tag{3}$$

where $\mathbf{B}_m$ is the current magnetic field and $\mathbf{B}^{mod}_m$ is best-fit model configuration for the current magnetic vector distribution. In all Doppler Imaging applications reconstruction of the surface distributions for sub-equatorial regions is less reliable, therefore we use additional weighting factor ω_m to prohibit strong contribution of those regions to the functional F_2.

With our modification of the regularization procedure MDI code has a tendency towards selecting magnetic field distribution close to the specified functional form, rather than just searching for the smoothest surface distribution like in conventional abundance or temperature mapping. New regularization does not depend on the method of search and parametrization of the optimal model field and therefore regularization procedure can be easily modified to use any prior knowledge about the type of magnetic field geometry expected for the particular class of objects. For modified version of `Invers10` we adopted low order multipolar field expansion which is known to give good results for magnetic CP stars:

$$\mathbf{B}^{mod} \approx -\nabla \left[\sum_{l=1}^{N} \sum_{n=-l}^{l} K^n_l S_{ln}(\theta,\phi) r^{-(l+1)} \right] \tag{4}$$

Coefficients K^n_l of the multipolar expansion into real spherical harmonics $S_{ln}(\theta,\phi)$ have to be determined by minimizing functional F_2 on every iteration. In fact for the general form of multipolar expansion (4) (as opposed to the expansion into axisymmetric harmonics $S_{l0}(\theta,\phi)$) K^n_l can be obtained from the system of linear equations

$$\frac{\partial F_2}{\partial K^n_l} = 0 \tag{5}$$

without introducing additional numerical minimization loop for every evaluation of the functional Q.

Multipolar regularization gives several important advantages over direct minimization of multipolar field parameters. First, is the possibility to fine-tune the strength of the preference to multipolar field by changing correspondent regularization parameter and

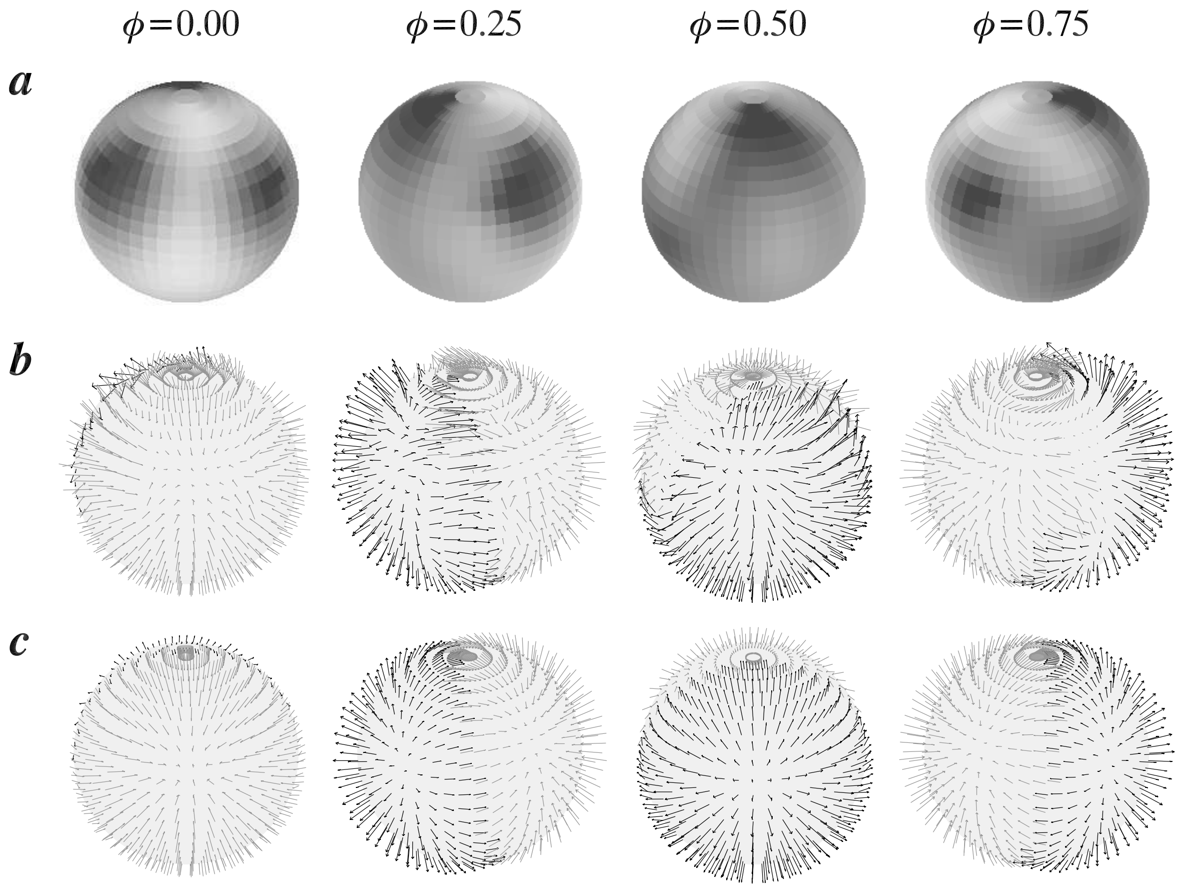

Figure 8: *MDI reconstruction of the surface Fe abundance (a) and vector magnetic field (b) distributions of α^2 CVn. Best-fit dipolar magnetic field is also shown (c).*

even switch it off in the case of complete Stokes vector dataset. Second, although with this regularization the code tends to select multipolar fields, it will not miss deviations from such fields, as long as these deviations influence line profiles and multipolar regularization parameter is selected properly. Third, new regularization conveniently provides an estimate of the multipolar field geometry on every iteration and allows to achieve better results for the reconstruction of the magnetic field in the low latitude surface regions.

To test the efficiency of multipolar regularization we conducted the same three reconstructions with different initial fields as on Fig. 6, but now first-order multipolar regularization was applied. Results appeared to be very satisfactory: for all three cases reconstructed magnetic distributions were virtually undistinguishable from the true magnetic map.

Multipolar regularization also automatically solved the problem of interpretation of MDI results obtained with `Invers10`. Before introducing new regularization the output of the code was just two-dimensional vector map, an array containing a few thousand numbers. In order to compare our results with the previous studies of particular stars we would need to translate numerical maps into multipolar field anyhow. Doing this parametrization via regularization is much more consistent solution than aposteriori fitting the resulting magnetic map.

4. Magnetic Imaging of α^2 CVn

Modified version of `Invers10` code was applied for the imaging of the prototype magnetic CP star α^2 CVn. This section briefly describes preliminary results of this first practical application of our MDI code.

Circular polarization observations that we used for the imaging were collected at the 2-m telescope of the Bulgarian National Astronomical Observatory at Rozhen. With the combination of Zeeman analyzer and CCD detector installed in the coude focus circular polarization spectra were obtained for 11 phases and 60 Å region around 5020 Å. Spectra have typical signal-to-noise ratio of 200 and resolution of 30000 (Fig. 9). Although this dataset has good phase coverage and signal-to-noise ratio, it is certainly not the best circular polarization data in terms of resolution and spectral coverage. This should be taken into account when discussing results of the magnetic field and abundance reconstruction. For the imaging we selected Fe II line at 5018.44 Å. It is one of the strongest

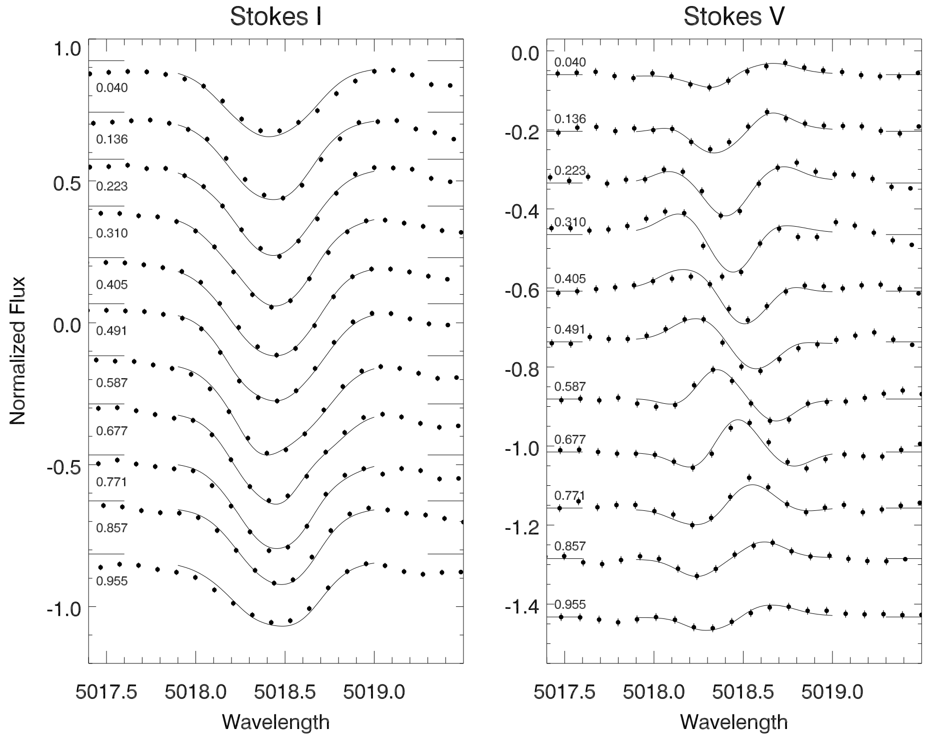

Figure 9: *Variations of Stokes I and V profiles for Fe* II *5018.44 Å in the spectrum of α^2 CVn. Observations are shown by circles and solid curves are predictions of the magnetic field and Fe abundance distribution model of Fig. 8.*

Table 2: *Numerical tests of the MDI code.*

Parameter changed	*Amount of change*	*Comments*
Field topology	$H_d = 0$ kG, $H_q = 8$ kG	
	$H_d = 8$ kG, $H_q = 8$ kG	
Abundance distribution	ring of enhanced abundance	
	several abundance spots	
Rotational velocity	$v \sin i = 20{,}10{,}5\ \mathrm{km\,s^{-1}}$	$\oplus$ for 5 $\mathrm{km\,s^{-1}}$
Inclination	$i = 30°$	$\oplus$
β angle	$\beta = 30°$	$\ominus$
Number of observations	10 phases	
Spectral resolution	R = 30000	
Error in the input parameters		
inclination	$i = 50, 70°$	
stellar $T_{\rm eff}$	$T_{\rm eff} = 8500$, 9500 K	
$v \sin i$	$v \sin i = 28$, 32 $\mathrm{km\,s^{-1}}$	$\oplus$
Type of observational data	Stokes I and V only	$\ominus$

$\oplus$: abundance map recovery problem
$\ominus$: magnetic field recovery problem

metal lines in α^2 CVn spectrum and has relatively large Landé factor. In solving inverse problem we used model atmosphere with parameters $T_{\rm eff} = 11500$ K, $log\,{\rm g} = 4.0$ and $[M/H] = +1.0$ from the study of Ryabchikova et al. (1999) and adopted $v \sin i = 17$ $\mathrm{km\,s^{-1}}$ and inclination $i = 50°$ used by Khokhlova & Pavlova (1985) in the abundance mapping of α^2 CVn.

Comparison between observed and computed Stokes I and V profiles is shown on Fig. 9. Fig. 8 displays results of the simultaneous abundance and magnetic field mapping. First order multipolar regularization was applied in this problem. Besides abundance and final magnetic field map best-fit dipolar magnetic configuration is also shown. Its parameters ($H_d = 5.26$ kG and $\beta = 100.6°$) are in very good agreement with the results of previous studies of α^2 CVn magnetic field (Borra & Landstreet 1977, Glagolevskij et al. 1985). Thus we conclude that

`Invers10` passed one more and probably the most realistic test.

Magnetic and abundance maps obtained for α^2 CVn is the first direct reconstruction of the vector distribution of magnetic field on CP star and the first result ever reported on the simultaneous recovering of the magnetic field vector and scalar abundance distributions. However bearing in mind relatively low resolution of the spectra that were used, we would like to postpone detailed discussion of the correlations between magnetic field and Fe abundance distribution until we will incorporate new high-quality circular polarization data into imaging of α^2 CVn. This work is currently underway.

Acknowledgements. It is author's pleasure to address grateful thanks to prof. N. Piskunov and Dr. T. Ryabchikova for stimulating discussions and help. This work was supported by Swedish Naturvetenskapliga forskningsrådet and Kungliga Vetenskapsakademien.

References

Borra E.F., Landsreet J.D., 1977, Astrophys. J., **212**, 141
Brown D., Landstreet J., 1981, Astrophys. J., **246**, 899
Brown S.F., Donati J.-F., Rees D.E., Semel M., 1991, Astron. Astrophys., **250**, 463
Donati J.-F., 1999, Mon. Not. R. Astron. Soc., **302**, 457
Glagolevskij Yu.V., Piskunov N.E., Khokhlova V.L., 1985, Pis'ma Astron. Zh., **11**, 371
Goncharsky A.V., Stepanov V.V., Khokhlova V.L., Yagola A.G., 1982, Astron. Zh., **59**, 1146
Johns-Krull C.M., Valenti J.A, 1996, Astrophys. J., **459**, L95
Khokhlova V.L., Pavlova V.M., 1984, Pis'ma Astron. Zh., **10**, 158
Mathys G., 1993, in: Peculiar versus Normal Phenomena in A-type and Related Stars, Dworestky M.M., Castelli F., Faraggiana R. (eds.), ASP Conf. Ser., **44**, 232
Piskunov N.E., 1985, Pis'ma Astron. Zh., **11**, 18
Piskunov N.E., 1999, in: 2nd Workshop on Solar Polarization, J.Stenflo and K.N.Nagendra (eds.), Bangalore, India, Kluwer Academic Publishers, Dodrecht, 515
Ryabchikova T., Piskunov N., Savanov I., Malanushenko V., 1999, Astron. Astrophys., **343**, 229
Semel M., 1989, Astron. Astrophys., **225**, 456
Strassmeier K.G., Linsky J.L. (eds.), 1996, IAU Symp. 176, Stellar Surface Structure, Kluwer Academic Publishers, Dodrecht
Vasilchenko D.V., Stepanov V.V., Khokhlova V.L., 1996, Pis'ma Astron. Zh., **22**, 924
Vogt S.S., Penrod G.D., Hatzes A.P., 1987, Astrophys. J., **321**, 496
Wade G.A., Donati J.-F., Landstreet J.D., Shorlin S.L.S., 1999, Mon. Not. R. Astron. Soc., in press